Journal of the Optical Society of Korea
Vol. 20, No. 6, December 2016, pp. 704-715

ISSN: 1226-4776(Print) / ISSN: 2093-6885(Online)
DOI: https://doi.org/10.3807/JOSK.2016.20.6.704

Bandwidth Allocation Under Multi-Level Service Guarantees of Downlink in the VLC-OFDM System

Shuangxing Liu, Xuefen Chi*, and Linlin Zhao

College of Communication Engineering, Jilin University, 5372, Nanhu Road, Changchun 130012, P. R. China

(Received July 13, 2016 : revised November 25, 2016 : accepted November 28, 2016)

In this paper, we explore a low-complex bandwidth allocation (BA) scheme with multi-level service guarantees in VLC-OFDM systems. Effective capacity theory, which evaluates wireless channel capacity from a novel view, is utilized to model the system capacity under delay QoS constraints of the link layer. Since intensity modulation of light is used in the system, problems caused by frequency selectivity can be neglected. Then, the BA problem can be formulated as an integer programming problem and it is further relaxed and transformed into a concave one. Lagrangian formulation is used to reformulate the concave problem. Considering the inefficiency of traditional gradient-based schemes and the demand for distributed implementation in local area networks, we localize the global parameters and propose a quasi-distributed quadratic allocation algorithm to provide two-level service guarantees, the first level is QoS oriented, and the second level is QoE oriented. Simulations have shown the efficient performance of the proposed algorithm. The users with more stringent QoS requirements require more subcarriers to guarantee their statistical delay QoS requirements. We also analyze the effect of subcarrier granularity on the aggregate effective capacity via simulations.

Keywords : Bandwidth allocation, VLC, OFDM, Effective capacity, Multi-level service guarantee
OCIS codes : (060.2605) Free-space optical communication; (060.4080) Modulation; (060.4510) Optical communications; (060.4256) Networks, network optimization

I. INTRODUCTION

The next generation communication networks are required to support high data rate services while guaranteeing multi-level quality of service (QoS) metrics, such as delay, value of service and a certain level of quality of experience (QoE) which is a widely used metric reflecting the users' satisfaction with the multimedia service. Due to the shortage of radio spectrum, traditional radio communication systems suffer from limited channel capacity. Compared to the radio-based wireless communication, visible light communication (VLC) brings multiple advantages such as greater bandwidth, higher data rate, being harmless to human bodies, ubiquitous data transmission and so on [1-3]. Orthogonal frequency division multiplexing (OFDM) which allows for parallel transmission on orthogonal subcarriers with a low-complexity transceiver [4] was introduced into VLC to improve data rate, mitigate the fading effects resulting from delay spread, and avoid low-frequency ambient interference [5]. In VLC-OFDM systems, the amplitude variation of the OFDM signal drives the intensity change of LED light. Once LED works in the non-linear region, the OFDM signal would be distorted. In this paper, we assume that LEDs are always working in their linear region. Because of the feature of weak penetration through obstacles and the short distance of data transmission, VLC is usually applied in indoor local area networks.

Most of the previous works about VLC-OFDM systems focused on the implementation and improvement of optical OFDM. Only a few works put their effort on the effective resource allocation algorithms. The authors in [6] have investigated the performance of a single carrier-frequency division multiple access (SC-FDMA) VLC system in the

*Corresponding author: chixf@jlu.edu.cn
Color versions of one or more of the figures in this paper are available online.

downlink of a multi-user data transmission system, and they jointly optimized the total transmission power and the subcarriers allocation for the VLC access point. The authors in [7] have analyzed the nonlinear clipping distortion of an asymmetrically clipped optical OFDM based VLC system and proposed an optimal power allocation method for reducing the clipping distortion. The authors in [8] have reported a novel asynchronous multiple access using a flexible bandwidth allocation scheme in the VLC system with 32/64QAM-OFDM, adopting quadrature amplitude modulation OFDM modulation. However, most previous works about resource allocation in VLC-OFDM systems neglected the delay in QoS demand of services.

In wireless networks, with the growing proliferation of delay-sensitive traffic, it is obligatory to support a wide variety of communication services with diverse delay QoS requirements. Nevertheless, it is tough to provide deterministic delay QoS guarantees in a wireless network because the wireless channel is varying all the time. The concept of statistical delay QoS in effective capacity theory has captured increasing attention of researchers. Effective capacity presents a novel perspective on the capacity of channels in terms of link-layer delay-QoS metric [9], which describes the supported maximum constant arrival rate of the system subject to the statistical delay-QoS constraint for a given service process.

In the study of radio frequency (RF) wireless communication systems with OFDM modulation, researchers have introduced the concept of statistical delay guarantees into their research [10]. The authors in [9] have developed an optimal strategy to maximize the throughput of the relay-based multiuser OFDMA systems with respect to the joint subchannel assignment and power control under both delay-QoS guarantees and average power constraints. The authors in [11] have proposed a delay QoS provision algorithm, which evolved an effective capacity model to capture the effect of channel fading on the queuing behavior of the link in wireless OFDM networks. The authors in [12] have investigated the resource allocation scheme for the uplink of the LTE network under statistical delay QoS guarantees. However, the previous works about resource allocation under statistical delay guarantees in RF-OFDM systems adopted the centralized scheme and required a coordinator with powerful functionality, which conflicts with the low-complexity design idea of coordinator in local area networks. Additionally, for the unipolar nature of VLC-OFDM signals, OFDM technique used in RF systems can't be applied in VLC systems directly.

We notice that the researchers in [13, 14] have the similar perspective with us in terms of statistical delay QoS guarantees in VLC systems. The authors in [13] have investigated the resource allocation algorithm under delay QoS constraints for heterogeneous visible-light and RF femtocell. The authors in [14] have proposed a novel QoS-driven non carrier sensing random access mechanism for the multi-packet reception-capable VLC system. However, we are different, we cope with the difficulties of discrete bandwidth allocation arising from the OFDM implemented in the VLC system and consider the specific problems of the optical channel. Furthermore, we try to support multi-level service guarantees in a simple way.

In this paper, we focus on the bandwidth allocation (BA) problem under the constraints of minimum bit rate, the maximum bandwidth usage efficiency and delay QoS guarantees in downlink of an indoor VLC-OFDM system. We propose a quasi-distributed BA scheme to provide multi-level service guarantees.

In OFDM system, bandwidth of the system is discretized as a bunch of subcarrier blocks (SBs). Intensity of light is modulated in the system, so the problem caused by frequency selectivity can be neglected. Therefore, the difference of VLC channel gain among SBs that are allocated to a user can be ignored. The BA problem can be formulated as an integer programming problem to decide the number of SBs allocated to each user with the target of maximizing the aggregate effective capacity. To solve the problem, we relax the integer constraints and reformulate the problem as a continuous optimization problem, where the optimum variables are defined as *ratio factors* indicating the percentage of bandwidth allocated to users. It's mathematically proved that the relaxed problem is concave with respect to *ratio factors*, which can be solved by convex optimization techniques.

Although gradient-based approaches have been proposed to solve the convex optimization problem, these schemes show many defects [12] such as oscillatory behavior, sensitivity to choice of initial values, etc. In our research, we target to support heterogeneous statistical delay QoS constraints, which inevitably aggravate the oscillatory behavior of gradient-based techniques. In addition, the conflict between guaranteeing minimum bit rate and maximizing bandwidth usage efficiency reduces the convergence rate of gradient-based schemes. Furthermore, the gradient-based approaches require high computational capability. It is essential to explore a simple and efficient BA algorithm. In this paper, we propose a quasi-distributed quadratic allocation scheme to lighten the burden of the coordinator by localizing the global parameters. We propose to provide multi-level service guarantees, we blend the statistical delay QoS guarantee with probability bandwidth request in the algorithm, the first one is QoS oriented, the second one is QoE oriented. We aim to create a space where an application can be tailored.

SB granularity refers to the size of a subcarrier in VLC-OFDM systems. In this paper, we also analyze the relationship between the bandwidth utilization and SB granularity via simulations.

The rest of the paper is organized as follows. In Section II, we describe the system model and channel model, and derive the expression of effective capacity of the VLC-OFDM system. The formulation of the BA problem is described in Section III. In Section IV, we propose a quasi-distributed BA scheme. The numerical and simulation results are shown in Section V. Finally, we make a conclusion in Section VI. The notations used in this paper are summarized in Table 1.

Table 1. The main symbol notation

l	Order of Lambertian emission
$\varphi_{1/2}$	Semi-angle at half power
A	Physical area of the photo-detector (PD)
Ts	Gain of the optical filter
ψ_{ir}	Angle of irradiation
ψ_{in}	Angle of incidence
$g(\psi_{in})$	Gain of an optical concentrator
n	Refractive index
Ψ_c	Width of the field of view (FOV)
ρ	Reflectance factor
ω1	Angle of irradiance to a reflective point
ω2	Angle of irradiance to a receiver
q	Electronic charge
τ	Detector's responsivity
B_e	Equivalent noise bandwidth
I_{bg}	Background current
r	Boltzmann's constant
G	Open-loop voltage gain
η	Fixed capacitance of the PD per unit area
Γ	FET channel noise factor
g_m	FET transconductance
I_1	Noise bandwidth factor
I_2	Noise bandwidth factor
T_k	Absolute temperature
B	Available bandwidth
R_k	Bit-rate constraint of user k
p	Block probability
L	Total number of RBs
P_t	Transmitted power

II. SYSTEM MODEL

In this paper, we consider the downlink of the VLC-OFDM system, as shown in Fig. 1. We focus on the resource allocation problem and consider that K users are distributed in the room. The users are indexed by $\mathbf{K} = \{1,\ldots,k,\ldots,K\}$. We consider heterogeneous delay QoS requirements that are characterized by a vector $\boldsymbol{\theta} = [\theta_k]_{K\times 1}$ with the element θ_k denoting the QoS exponent in effective capacity theory of the user k, $k \in \mathbf{K}$.

We assume that all users are stationary while there are moving obstructions in the room, such as human beings, which might block the LOS links of downlinks. The OFDM technique is utilized in the downlink transmission of the VLC system [3] to achieve parallel communications. The available bandwidth B is divided into L SBs with equivalent bandwidth [3]. The SBs are indexed by the set $\mathbf{L} = \{1,\ldots,l,\ldots,L\}$. SB granularity ϖ, which is referred as the size of an SB, is the basic unit while allocating bandwidth. An IM/DD (intensity modulation/direct detection) technique is used in the system, which implies that the phase information is lost and only the intensity of LED light is modulated with data. Therefore, the transmitted signal must be positive real, and at least half of the SBs must be used to realize the Hermitian conjugate of the complex-valued symbol after modulation. Consequently, at most half of the bandwidth can be exploited for signal transmission [15].

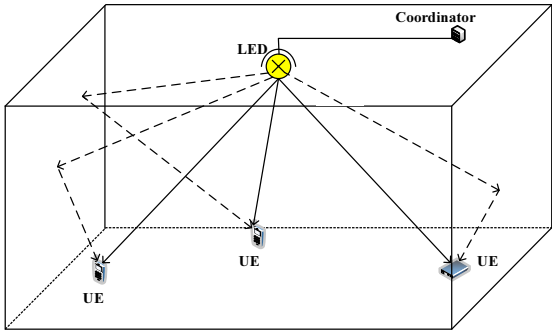

FIG. 1. An indoor VLC-OFDM scenario.

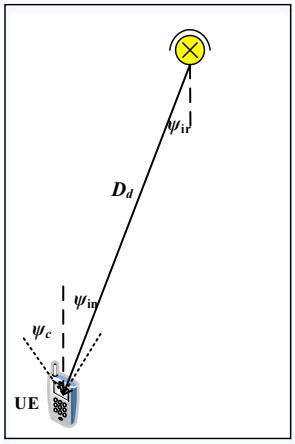

FIG. 2. VLC LOS channel model.

2.1. Channel Model

In the VLC system, signals are detected by a photo-detector (PD) at the receiver. The received signals are a mix of direct portion with single/multiple reflected portion [18]. The direct portion is called the-line-of-sight (LOS) signal, which provides high channel gain but is vulnerable to interruption. Otherwise, the non-line-of-sight (NLOS) signal, which has lower channel gain but is robust to environmental change. In this paper we will consider both LOS signal and NLOS signals on the first reflection [13, 16, 17].

In an optical LOS channel, as shown in Fig. 2, the direct current (DC) gain is given as [13]:

$$H(0)=\begin{cases}\dfrac{(La+1)AT_s\kappa}{2\pi D_d^2}\cos^{La}(\psi_{ir})g(\psi_{in})\cos(\psi_{in}), & if\ \psi_{in}\le\psi_c\\ 0, & if\ \psi_{in}>\psi_c\end{cases}$$

where A is the physical area in a PD, D_d is the distance between a transmitter and a receiver, ψ_{ir} is the angle of

irradiation of the LED lights, ψ_{in} is the angle of incidence, ψ_c denotes the width of the field of view (FOV) at the receiver, *T*s is the gain of the optical filter used, and *La* is the order of Lambertian emission which is given by the semi-angle $\phi_{1/2}$ at half illumination of an LED as [17]:

$$La = \frac{\ln 2}{\ln(\cos \phi_{1/2})}$$

$g(\psi_{in})$ denotes the gain of an optical concentrator [18] [19]:

$$g(\psi_{in}) = \begin{cases} \dfrac{La^2}{\sin^2 \psi_c}, & if\ \psi_{in} \le \psi_c \\ 0, & if\ \psi_{in} > \psi_c \end{cases}$$

The VLC LOS channel might be blocked by obstructions. The blocking event is represented by a random variable κ, $\kappa = 1$ if the LOS channel is blocked, otherwise $\kappa = 0$. We assume that κ obeys the Bernoulli distribution [13]. The LOS channel is blocked with probability p_k which is decided by the communication scenario and the location of user k. The probability mass function of κ for user k is expressed as:

$$f_k(\kappa) = \begin{cases} p_k, & if\ \kappa = 1 \\ 1 - p_k, & if\ \kappa = 0 \end{cases}$$

The received optical power is given by the DC gain on the LOS path $H(0)$ and the first reflected paths $H_{ref}(0)$, which may be written as [17]:

$$p_r = p_t H(0) + \int_{walls} p_t dH_{ref}(0)$$

P_t and P_r denote the transmitted and received power respectively. The channel DC gain of the first reflection is characterized by [17]:

$$dH_{ref}(0) = \begin{cases} \dfrac{(l+1)AT_s\rho}{2\pi D_1^2 D_2^2} J \cos^l(\psi_{ir}) g(\psi_{in}) \cos(\psi_{in}) dA_{walls} & if\ \psi_{in} \le \psi_c \\ 0 & if\ \psi_{in} > \psi_c \end{cases}$$

where D_1 denotes the distance between the user and a reflecting surface, D_2 denotes the distance between the reflective point and the receiver, ρ is the reflectance factor, whilst dA_{walls} is a small reflective area, and J=cos(ω_1) cos (ω_2), where ω_1 and ω_2 denote the angle of irradiance to a reflective point and the angle of irradiance to the receiver respectively. The first reflective channel model is shown in Fig. 3.

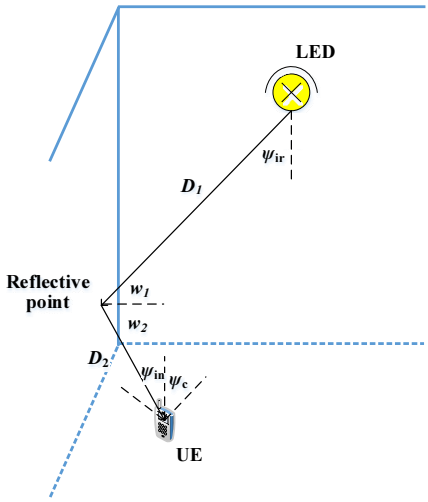

FIG. 3. The first reflective channel model.

We consider both shot noise and thermal noise [13, 17]. Hence, the Gaussian noise has a total variance of σ^2, which is the sum of shot noise and thermal noise:

$$\sigma^2 = \sigma^2_{shot} + \sigma^2_{thermal}$$

The variance of shot noise σ^2_{shot} is given by [18]:

$$\sigma^2_{shot} = 2q\tau P_r B_e + 2qI_{bg} I_1 B_e$$

where q is the electronic charge, τ is the detector's responsivity. B_e is the equivalent noise bandwidth. I_{bg} is the background current caused by the background light. The variance of thermal noise is given by [17]:

$$\sigma^2_{thermal} = \frac{8\pi r T_k}{G} \eta A I_1 B_e^2 + \frac{16\pi^2 r T_k \Gamma}{g_m} \eta^2 A^2 I_2 B_e^3$$

where r is the Boltzmann's constant, T_k is the absolute temperature, G is the open-loop voltage gain, η is the fixed capacitance of the PD per unit area, Γ is the FET channel noise factor, and finally, g_m is the FET transconductance. The noise bandwidth factors I_1 and I_2 are constant experimental values.

The SNR at the receiver for user k on SB l, where $k \in \mathbf{K}$, $l \in \mathbf{L}$, is denoted by $\gamma_{k,l}$:

$$\gamma_{k,l} = \frac{(\tau P^k_{r,l})^2}{\sigma^2_{k,l}}$$

According to the Shannon capacity equation, the upper bound of the achievable data rate for user k on the SB l is given by:

$$R_{k,l} = \varpi \log_2(1+\gamma_{k,l})$$

where $\varpi = \frac{B}{L}$ is SB granularity. As discussed above, at most half of the bandwidth can be exploited for signal transmission, we can get the upper bound of the achievable data rate for user k, which can be expressed as:

$$R_k = \sum_{l=1}^{L} z_{k,l} \frac{\varpi}{2} \log_2(1+\gamma_{k,l})$$

where $z_{k,l} \in \{0,1\}$, $z_{k,l} = 1$ if user k occupies SB l, otherwise $z_{k,l} = 0$.

Since an IM/DD technique is utilized, there is no explicit carrier of a single frequency but the intensity of light is modulated [3]. In this respect, the problem caused by frequency selectivity can be neglected. In addition, the VLC channel is modeled as a two-rate channel in which the DC gain is affected by the position, blocking situation, and the corresponding physical parameters of VLC channels such as FOV. Therefore, there is no difference of channel DC gain among SBs allocated to a user. We assume that L_k SBs are allocated to user k, and for any SB i allocated to user k, we have $\gamma_k = \gamma_{k,i}$. The achievable data rate for user k can be rewritten as:

$$R_k = L_k \frac{\varpi}{2} \log_2(1+\gamma_k) \tag{1}$$

2.2. Effective Capacity of VLC

Effective capacity theory, which was proposed by Wu and Negi in 2003 [20], is the dual problem of effective bandwidth. It characterizes the maximum constant arrival rate of a given service process under the statistical delay QoS constraint. The QoS exponent θ describes the steady state delay violation probability, the expression is shown as $Pr\{d > d^T\} = e^{-\theta\varphi d^T}$, where d is the steady state delay, d^T is the delay bound, and φ is determined by the arrival and service processes [21]. It should be noted that a smaller θ indicates a looser QoS constraint whereas a larger θ implies a more stringent QoS constraint.

The effective capacity [12, 20] for user k is given by:

$$C_E^k(\theta_k, \varpi; z_{k,l}) = -\frac{1}{\theta_k} \ln E(e^{-\theta_k R_k}) \tag{2}$$

The instantaneous data rate can be expressed as [13]:

$$R_k = \begin{cases} \Re_{1,k}, & \text{with probability } 1-p_k \\ \Re_{2,k}, & \text{with probability } p_k \end{cases}$$

where $\Re_{1,k}$ and $\Re_{2,k}$ denote the achievable transmission rate for user k with and without VLC LOS reception, respectively. Therefore, the effective capacity for user k is given by:

$$C_E^k(\theta_k, \varpi; z_{k,l}) = \begin{cases} -\frac{1}{\theta_k} \ln((1-p_k)e^{-\theta_k \Re_{1,k}} + p_k e^{-\theta_k \Re_{2,k}}), & if\ \psi_{in} \le \psi_c \\ 0, & if\ \psi_{in} > \psi_c \end{cases} \tag{3}$$

III. PROBLEM FORMULATION

The bandwidth allocation problem is formulated as the maximization of aggregate effective capacity, which can be expressed as:

$$\max_{\mathbf{L}} \ C_E(\boldsymbol{\theta}, \varpi; \mathbf{L}) \qquad \text{(Problem 1)}$$
$$s.t \quad (a) \quad C_E^k(\theta_k, L_k) \ge R_k \quad k \in \mathbf{K}$$
$$(b) \quad 1^{\mathrm{T}}\mathbf{L} = \mathrm{L}$$

The objective of the optimization Problem 1 is to find a SBs allocation strategy to maximize the aggregate effective capacity under specific statistical delay constraints. $\mathbf{L} = [L_k]_{Kx1}$, $k \in \mathbf{K}$, is the SBs indicated matrix which satisfies $1^{\mathrm{T}}\mathbf{L} = \mathrm{L}$. The aggregate effective capacity of the VLC system, defined as $C_E(\boldsymbol{\theta}, \varpi; \mathbf{z})$, is given by:

$$C_E(\boldsymbol{\theta}, \varpi; \mathbf{z}) = \sum_{k=1}^{K} C_E^k \tag{4}$$

Physically, constraint (a) guarantees the minimum bit-rate requirement for user k. Constraint (b) physically ensures the maximum bandwidth utilization.

Problem 1 is an integer non-linear programming problem. A solution to solve an integer programming problem is to relax the integer constraint. Certainly, Problem 2 is not actually solved by the relaxation of the integer constraint. However, it has been shown in [22] that solving the dual of the relaxed problem provides solutions that are arbitrarily close to the original, non-relaxed problem [13].

$\underline{L}_k$ denotes the bandwidth allocated to user k, it is a continuous variable in the interval [0, L]. Let $\beta_k = \underline{L}_k/L$, where $k \in \mathbf{K}$., β_k is the *ratio factor* for user k which is a continuous variable in the interval [0, 1]. The achievable data rate for user k is rewritten as:

$$R_k = \beta_k \frac{\varpi L}{2} \log_2(1+\gamma_k)$$

Next, let $R_{1,k} = \frac{\varpi L}{2} \log_2(1+\gamma_{1,k})$, $R_{2,k} = \frac{\varpi L}{2} \log_2(1+\gamma_{2,k})$,

where $\gamma_{1,k}$ and $\gamma_{2,k}$ denotes the SNRs for user k with and without LOS reception, respectively. So the effective capacity for user k given by (3) can be expressed as:

$$C_E^k(\theta_k,\varpi;\beta_k)=\begin{cases}-\frac{1}{\theta_k}\ln((1-p_k)e^{-\theta_k\beta_k R_{1,k}}+p_k e^{-\theta_k\beta_k R_{2,k}}), & if\ \psi_{in}\le\psi_c\\ 0, & if\ \psi_{in}>\psi_c\end{cases} \tag{5}$$

Then, the relaxed optimization problem of Problem 2 could be reformulated as follows:

$$\begin{aligned}&\max_{\boldsymbol{\beta}}\ C_E(\boldsymbol{\theta},\varpi;\boldsymbol{\beta}) && \text{(Problem 2)}\\ &s.t\ \ (a)\ \ C_E^k(\theta_k)\ge R_k && \forall k\in\mathbf{K}\\ &\quad\ (b)\ \ \textstyle\sum_{k=1}^{K}\beta_k=1 && k\in\mathbf{K}\\ &\quad\ (c)\ \ 0\le\beta_k\le 1 && \forall k\in\mathbf{K}\end{aligned}$$

where $\boldsymbol{\beta}=[\beta_k]_{K\times 1}$ denotes the SBs allocation matrix. Constraint (b) involves the sum of β_k, it is a global constraint to ensure the maximum bandwidth usage efficiency. Constraint (a) is a local constraint that guarantees the minimum bit rate requirement for each user.

Lemma 1: Problem 2 is a concave optimization problem.

Proof: See Appendix A.

IV. A QUASI-DISTRIBUTED ALGORITHM

Problem 2 may be solved with the aid of centralized tools which require a coordinator with powerful functionality, which runs contrary to the low-complexity design idea of coordinator in local area networks. It may be appropriate to apply distributed tools to find the solution. Nevertheless, it is difficult to achieve completely distributed algorithms. Traditional gradient-based algorithms show many defects such as oscillatory behavior, sensitivity to choice of initial values, etc. In our research, we aim to support heterogeneous statistical delay QoS constraints which inevitably aggravate the oscillatory behavior of gradient-based techniques. Moreover, the conflict between guaranteeing minimum bit rate and maximizing bandwidth utilization reduces the convergence rate of gradient-based schemes. It is essential to explore a simple and efficient BA algorithm. In this section, we propose a quasi-distributed quadratic BA algorithm, the first one is QoS oriented, and the second one is QoE oriented.

As discussed in Section III, Problem 2 is a concave one which implies that we can use Lagrangian formulation to reformulate the optimization problem [22]. The Lagrangian function of Problem 2 with constraints (a)-(c) is expressed as:

$$L(\boldsymbol{\theta},\varpi;\boldsymbol{\beta},\lambda,\boldsymbol{\mu})=C_E(\boldsymbol{\theta},\varpi;\boldsymbol{\beta})-\lambda(\textstyle\sum_{k=1}^{K}\beta_k-1)-\sum_{k=1}^{K}\mu_k(R_k-C_E^k)$$

where $\lambda\ge 0$ and $\mu_k\ge 0$, $k\in\mathbf{K}$, are the Lagrange multipliers. We define λ as the global multiplier and μ_k as the local multiplier. The objective function in Problem 2 can be written as:

$$C_E(\boldsymbol{\theta},\varpi;\boldsymbol{\beta})=\min_{\boldsymbol{\lambda},\boldsymbol{\mu}} L(\boldsymbol{\theta},\varpi;\boldsymbol{\beta},\lambda,\boldsymbol{\mu})$$

The maximum of $C_E(\boldsymbol{\theta},\boldsymbol{\beta})$ can be expressed as:

$$\max_{\boldsymbol{\beta}} C_E(\boldsymbol{\theta},\varpi;\boldsymbol{\beta})=\max_{\boldsymbol{\beta}}\min_{\boldsymbol{\lambda},\boldsymbol{\mu}} L(\boldsymbol{\theta},\varpi;\boldsymbol{\beta},\lambda,\boldsymbol{\mu}) \tag{6}$$

According to Karush-Kuhn-Tucker (KKT) conditions, when the following two conditions is satisfied:

$$\lambda=0\ \ or\ \ \textstyle\sum_{k=1}^{K}\beta_k-1=0 \tag{7}$$

$$\mu_k=0\ \ or\ \ R_k-C_E^k=0,\ \forall k\in\mathbf{K} \tag{8}$$

we have the following equations:

$$\begin{aligned}\max_{\boldsymbol{\beta}} C_E(\boldsymbol{\theta},\varpi;\boldsymbol{\beta})&=\max_{\boldsymbol{\beta}}\min_{\boldsymbol{\lambda},\boldsymbol{\mu}} L(\boldsymbol{\theta},\varpi;\boldsymbol{\beta},\lambda,\boldsymbol{\mu})\\ &=\min_{\boldsymbol{\lambda},\boldsymbol{\mu}}\max_{\boldsymbol{\beta}} L(\boldsymbol{\theta},\varpi;\boldsymbol{\beta},\lambda,\boldsymbol{\mu})\end{aligned}$$

which implies that the optimal SBs allocation matrix $\boldsymbol{\beta}^*$ can be obtained by solving :

$$\min_{\boldsymbol{\lambda},\boldsymbol{\mu}}\max_{\boldsymbol{\beta}} L(\boldsymbol{\theta},\varpi;\boldsymbol{\beta},\lambda,\boldsymbol{\mu}) \tag{9}$$

The dual objective function $g(\lambda,\boldsymbol{\mu})$ is defined as the maximum value of the Lagrangian function over $\boldsymbol{\beta}$, which can be expressed as:

$$g(\boldsymbol{\theta},\varpi;\lambda,\boldsymbol{\mu})=\max_{\boldsymbol{\beta}} L(\boldsymbol{\theta},\varpi;\boldsymbol{\beta},\lambda,\boldsymbol{\mu})$$

Eq. (9) can be expressed as the minimum of $g(\lambda,\boldsymbol{\mu})$ which is described as:

$$\begin{aligned}&\min_{\boldsymbol{\lambda},\boldsymbol{\mu}} g(\boldsymbol{\theta},\varpi;\lambda,\boldsymbol{\mu})\\ &\text{sub}\ \ \lambda\ge 0,\boldsymbol{\mu}\ge 0\end{aligned} \tag{10}$$

Eq. (10) is always a convex optimization problem. There is a duality gap between the optimal primal objective expressed in Problem 2 and its optimal dual objective Eq. (10), which is always nonnegative [13]. According to the central result in convex analysis that the duality gap reduces to zero at the optimum, when the problem is convex [22, 23]. Therefore, the primal problem can be equivalently solved

by solving the dual problem of Eq. (10).

To solve problem Eq. (10), we take λ and $\boldsymbol{\mu}$ as constants, and obtain the optimal $\boldsymbol{\beta}^*$, which can be written as:

$$\boldsymbol{\beta}^* = \arg \max_{0 \le \boldsymbol{\beta} \le 1} L(\boldsymbol{\theta}, \varpi; \boldsymbol{\beta}, \lambda, \boldsymbol{\mu})$$

The second derivative of $L(\boldsymbol{\beta}, \lambda, \boldsymbol{\mu})$ with respect to β_k, $k \in \mathbf{K}$, is expressed as:

$$\frac{\partial^2 L(\boldsymbol{\beta}, \lambda, \boldsymbol{\mu})}{\partial \beta_k^2} = C_E^{k''} + u_k C_E^{k''}$$

As discussed in Appendix A, we have $C_E^{k''} \le 0$, and μ_k is greater than zero, we have $\frac{\partial^2 L(\boldsymbol{\beta}, \lambda, \boldsymbol{\mu})}{\partial \beta_k^2} \le 0$, which implies that $L(\boldsymbol{\beta}, \lambda, \boldsymbol{\mu})$ is concave with respect to β_k. The optimal β_k^* may be achieved by solving [7]:

$$\frac{\partial L(\boldsymbol{\beta}, \lambda, \boldsymbol{\mu})}{\partial \beta_k} = C_E^{k'} - \lambda + \mu_k C_E^{k'} = 0 \tag{11}$$

Next, we utilize β_k^* to update λ and $\boldsymbol{\mu}$. To achieve distributed implementation and increase the convergence rate, we localize the global multiplier λ into local parameters.

According to (11), we have:

$$C_E^{k'} = \frac{\lambda}{1+\mu_k} \tag{12}$$

Observed from Eq. (12), the optimal β_k^* is a function of $\frac{\lambda}{1+\mu_k}$. Instead of updating λ and $\boldsymbol{\mu}$ respectively, which contributes to a slow convergence rate, we update $\frac{\lambda}{1+\mu_k}$ directly. We let $A_k = \frac{\lambda}{1+\mu_k}$. According to Appendix B, The feasible region of A_k is $[\frac{p_k R_{2,k} + \xi(1-p_k) R_{1,k}}{p_k + \xi(1-p_k)}, p_k R_{2,k} + (1-p_k) R_{1,k}]$, where $\xi = e^{-\theta(R_{1,k} - R_{2,k})}$. We assume that $0 < p < 1$, the closed-form of β_k^* can be described as:

$$\beta_k^* = \frac{1}{-\theta_k (R_{1,k} - R_{2,k})} \ln \frac{p_k (A_k - R_{2,k})}{(1-p_k)(R_{1,k} - A_k)} \tag{13}$$

The proof of Eq. (13) can be seen in Appendix B. Based on Eq. (13), we can adjust the bandwidth allocated to user k through changing the value of A_k.

To find the optimal A_k, we firstly take A_k as constants, and get the corresponding optimal β_k^*. Then we use β_k^* to update A_k, after that we use the newly A_k to obtain the newly β_k^*. This process continues until β_k^* converges or reaches the maximum iterations. A_k is updated according to:

$$A_k(t+1) = A_k(t) + Step_k(t) f_k(1 - \sum_{k=1}^{K} \beta_k^*) \tag{14}$$

where $Step_k(t)$ is the iterative step function, the value of which is not smaller than zero. $f_k(1 - \sum_{k=1}^{K} \beta_k^*)$ is the iterative direction function which determines to increase or decrease A_k, and it takes the value of -1, 0, or 1.

Next, we investigate the iterative step function which guarantees the convergence of A_k after finite iterations. The iterative step is described as:

$$step_k(t) = \begin{cases} step_k(t) + \Delta s(t), & if\ f_k(t) = f_k(t_k) \\ step_k(t) - \Delta s'(t), & if\ f_k(t) \ne f_k(t_k) \\ step_k(t_k), & if\ f_k(t) = 0 \end{cases} \tag{15}$$

where $f_k(t)$ is the iteration direction of the tth iteration for user k. Δs and $\Delta s'$ are the increments of iteration step which are not smaller than zero. $f_k(t_k)$ is the last iteration direction when $f_k(t_k)$ is not equal to zero. The optimal solution is sensitive to the initial value of $step_k(t)$. In this paper, we let:

$$step_{k,ini} = \frac{p_k R_{2,k} + \xi(1-p_k) R_{1,k}}{p_k + \xi(1-p_k)} - A_{k,ini}$$

Then, we explore the iterative direction function. To achieve the maximum bandwidth efficiency, the sum of β_k^* should be close to one. According to Appendix B, β_k^* is monotonic decreasing with A_k. After the current iteration, if the sum of β_k^* is less than one, there would be extra bandwidth that remained in the system. And all users can still attempt to increase their *ratio factors* by decreasing A_k in the next iteration. On the contrary, if the sum of β_k^* is greater than one after the current iteration, all users would have to decrease their *ratio factors* by increasing A_k. The iteration direction function for user k can be described as:

$$\begin{aligned} &if\ \ 1 - \sum_{k=1}^{K} \beta_k^* \ge \varpi, \\ &\quad f_k(1 - \sum_{k=1}^{K} \beta_k^*) = \begin{cases} -1 & with\ probability\ \alpha_k \\ 0 & with\ probability\ (1-\alpha_k) \end{cases} \\ &if\ \ 1 - \sum_{k=1}^{K} \beta_k^* < 0, \\ &\quad f_k(1 - \sum_{k=1}^{K} \beta_k^*) = 1 \\ &if\ \ 0 \le 1 - \sum_{k=1}^{K} \beta_k^* < \varpi, \\ &\quad f_k(1 - \sum_{k=1}^{K} \beta_k^*) = 0 \end{aligned} \tag{16}$$

Eq. (16) illustrates that the *ratio factors* would not be changed anymore when less than one SB is remained to be allocated in the system. α_k is the bandwidth request probability for user k which reflects user's QoE requirements. The introduction of α_k into the algorithm provides a space for multi-level service guarantees.

The BA algorithm is a quadratic allocation one. The first one is QoS oriented. We allocate bandwidth to each user to guarantee their minimum bit rate requirement. A_k is initialized to the value of guaranteeing the minimum bit rate requirement of user k. For each user k, we let $C_E^k(\beta_k) = R_k$. We can obtain the minimum *ratio factor* $\beta_{k,ini}$ through the binary search method. $\beta_{k,ini}$ indicates the minimum bandwidth for user k to guarantee their minimum bit rate requirement. Based on Eq. (13), we can get $A_{k,ini}$. $A_{k,ini}$ is also the upper bound to ensure minimum bit rate requirement. The second one is QoE oriented. We allocate the remainder bandwidth to users based on their bandwidth request probability. A bigger bandwidth request probability for user k implies a larger probability to allocate more bandwidth to use k.

Figure 4 illustrates how the algorithm works. We assume that α_k is equal to one. After the tth iteration, A_k changes from $A_{k,t-1}$ to $A_{k,t}$, the iterative direction $f(t) = -1$, the iterative step is step(t). In the $(t+1)$th iteration, if $f(t) \neq f(t+1)$ which means that the optimal A_k falls into region 1, we obtain the $(t+1)$th iterative step according to expression Eq. (15). We assume that after the $(t+1)$th iteration, A_k changes from $A_{k,t}$ to $A_{k,t+1}$, as shown in Fig. 4. Next, we compare the value of $f(t+2)$ and $f(t+1)$. If $f(t+2)$ is not equal to $f(t+1)$, the optimal A_k falls into region 2, if $f(t+2)$ is equal to $f(t+1)$, the optimal A_k falls into region 3. Each iteration makes A_k get closer to the optimal solution.

Based on the above discussions, the quasi-distributed BA scheme is constituted by an iterative algorithm which searches for the optimal *ratio factors* based on the update of A_k. A_k is initialized to a feasible value $A_{k,ini}$, the optimal *ratio factors* are calculated based on Eq. (13) at the user side. Then, coordinator calculates the value of $1-\sum_{k=1}^{K}\beta_k^*$ and broadcasts the calculated result to each user. After that, each user obtains its iterative direction function based on Eq. (16). Next, users calculate its iterative step function according to Eq. (15) based on the new value of iterative direction function, and then update A_k according to Eq. (14). This process continues until convergence. The quasi-distributed BA scheme is formally described in Table 2.

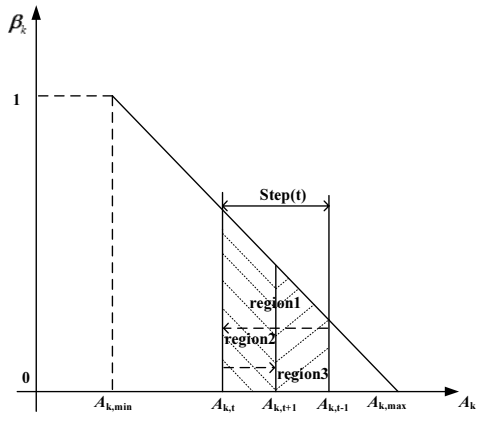

FIG. 4. Illustration of quasi-distributed BA algorithm.

After obtaining the optimal ratio factors, we discretize the bandwidth allocated to each user into the integral multiple of SB granularity. Firstly, based on β_k^* and L, we obtain $\underline{L}_k$. And then we discretize $\underline{L}_k$ through the equation:

$$L_k^* = \begin{cases} \lfloor L\beta_k^* \rfloor, & C_E^k(L_k^*) \geq R_k \\ \lceil L\beta_k^* \rceil, & C_E^k(L_k^*) < R_k \end{cases} \tag{17}$$

where L_k^* is the number of SBs allocated to user k, $k \in \mathbf{K}$. Operator $\lfloor\ \rfloor$ is the rounding down operator, and operator $\lceil\ \rceil$ is the rounding up operator. The achievable data rate for user k after discretization is given by:

$$R_k = L_k^* \frac{\varpi}{2} \log_2(1+\gamma_k) \tag{18}$$

TABLE 2. The quasi-distributed BA scheme

Input
θ_k : Delay requirement of each user k, k = 1,2,…,K
R_k: Rate requirement of each user k, k = 1,2,…,K
p_k: Blocking probability of each user k, k = 1,2,…,K
α_k: Bandwidth request probability of each user k, k = 1,2,…,K

Initialzation
t←1
for each user
$A_k(t) = A_{k,ini}$
End for

While t dose not reach its maximum
  Get optimal β_k
  For each user k
    User k solve the problem presented in Eq. (13)
  End for
  If sum(β_k) < ϖ
    Break;
End if
  Update A_k
  For each user k
    Iterative direction is updated according to Eq. (16);
Iterative step is updated according to Eq. (15);
    A_k is updated according to Eq. (14);
  End for
  t = t+1
End while
  For each user k
    $L_k = \lfloor L\ \beta_k \rfloor$;
  End for

Output $\underline{L}$

According to (4), (5) and (18), we obtain the aggregate effective capacity.

V. NUMERICAL AND SIMULATION RESULTS

Our simulation model is based on the downlink transmissions of a multi-user VLC-OFDM system, shown in Fig. 1. The two-rate transmission channel model is used. We assume that 10 terminals which are divided into three groups are uniformly distributed in the room, the users in the same group experience the same delay QoS requirements while the users in different groups experience heterogeneous delay QoS requirements. The main system parameters are given in Table 3.

Figure 5 demonstrates the convergence behavior of the quasi-distributed BA scheme in different blocking situations where the VLC blocking probabilities are 0.1, 0.2 and 0.5 respectively. We assume that all users experience the same QoE requirement, and for any $k \in \mathbf{K}$, we let α_k be equal to 0.8. As shown in Fig. 5, the BA algorithm which indeed finds the *ratio factors* converges to the optimal value within 20 iterations.

TABLE 3. Simulation configuration parameters

Length of room	5 m
Height of room	3 m
Height of LED	2.5 m
Location of LEDs	(2.5,1.25,2.5), (2.5,3.75,2.5)
Semi-angle at half power	70 deg
Physical area of the photo-detector (PD)	1 cm^2
Gain of the optical filter	1.0
Refractive index	1.5
Width of the field of view (FOV)	60 deg
Reflectance factor	0.8
Electronic charge	1.6×10^{-19} C
Detector's responsivity	0.54 A/W
Equivalent noise bandwidth	10 Mbps/L
Background current	5.1×10^{-3}A
Boltzmann's constant	1.38e-23
Open-loop voltage gain	10
Fixed capacitance of the PD per unit area	112
FET channel noise factor	1.5
FET transconductance	3×10^{-2} s
Noise bandwidth factor	0.562
Noise bandwidth factor	0.0868.
Absolute temperature	295 k
Available bandwidth	20 MHz
Bit-rate constraint	5/10/15 Mbps
Block probability	0.2
Number of RBs	512
Transmitted power	1 W

Figure 6 illustrates the effect of the delay exponent θ on the aggregate effective capacity. We compare the performance between the proposed BA scheme and the average bandwidth allocation scheme when the blocking probabilities are 0.2 and 0.5, respectively. We assume that all users experience the same delay exponents, and the same QoE requirement. For any $k \in \mathbf{K}$, we let α_k be equal to 0.8. Observed from Fig. 6, the BA scheme can reach a greater aggregate effective capacity than the average bandwidth allocation scheme does, and the advantages of the BA scheme would be greater as the QoS requirement becomes more stringent. In addition, the aggregate effective capacity is reduced upon increasing the delay exponent θ, the VLC system is sensitive to the delay constraints, and the total effective capacity degrades rapidly for $\theta \geq 0.1$.

Figure 7 demonstrates the *ratio factors* versus the user index at a 0.2 VLC blocking probability, in conjunction

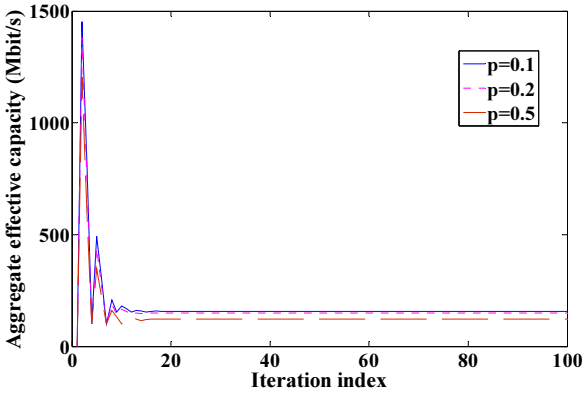

FIG. 5. The aggregate effective capacity values versus the total number of iterations.

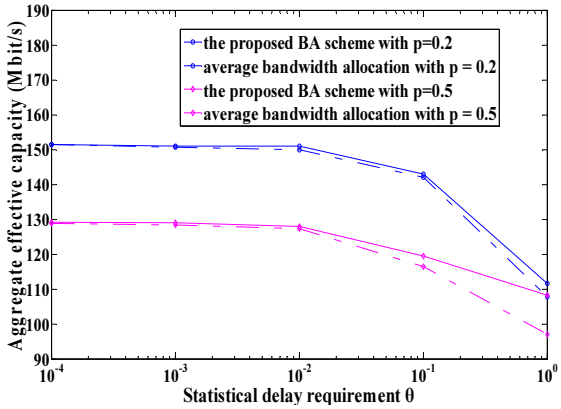

FIG. 6. The aggregate effective capacity versus the statistical delay exponent.

with $\theta = 0.001$ for users in group 1, $\theta = 0.01$ for users in group 2 and $\theta = 0.1$ for users in group 3. We assume that all users experience the same QoE requirement, and for any $k \in \mathbf{K}$, we let α_k be equal to 0.8. Observed from Fig. 7, almost the same number of SBs are allocated to the users with the same delay exponents. The slight difference among different users in the same group is mainly caused by the different positions. Furthermore, more SBs are assigned to the users with larger delay exponent θ, which implies a more stringent QoS requirement, to guarantee their delay QoS constraint. Figure 8 shows the numbers of SBs allocated to each user.

Figure 9 demonstrates the effect of bandwidth request probability $\boldsymbol{\alpha}$ of the users in group 3 on the effective capacity. We assume that $\theta = 0.001$ for users in group 1, $\theta = 0.01$ for users in group 2 and $\theta = 0.1$ for users in group 3. And the users in group 1 and group 2 experience the same QoE requirement. For any user k in group 1 and group 2, we let $\alpha_k = 0.6$. Additionally, the VLC blocking probability is 0.2. Observed from Fig. 9, since a greater bandwidth request probability for user k implies higher probability to allocate SBs to user k, with increasing the bandwidth request probability of group 3 the effective capacity of group 3 is raised. However, because the system bandwidth is fixed, the bandwidth allocated to the users in group 1 and group 2 decrease, so the aggregate effective capacity of group 1 and group 2 decreases. Additionally, the aggregate effective capacity of group 1, group 2 and group 3 remains almost the same as the bandwidth request probability of group 3 increases. It implies that the bandwidth request probability just affects the distribution of SBs, but has no effect on the aggregate effective capacity of the system. Moreover, as shown in Fig. 9, even if the bandwidth request probability of the users in group 3 is zero, there still are SBs allocated to the users in group 3. This is because the proposed algorithm primarily allocates bandwidth to users to satisfy their minimum bit rate requirements.

Figure 10 shows the effect of SB granularity on the aggregate effective capacity before and after discretization of $\underline{L}_k$ in the situation that the VLC blocking probabilities are 0.2 and 0.5, respectively. We assume that all users experience the same delay exponents, the system bandwidth B is 20 MHz. And all users have the same bandwidth request probability, for any $k \in \mathbf{K}$, we let α_k be equal to 0.8. As Fig. 10 shows, the aggregate effective capacity

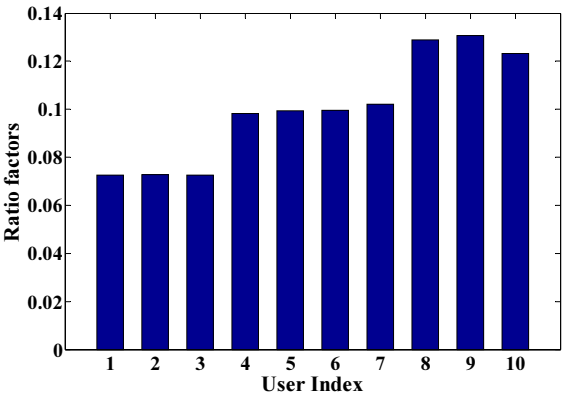

FIG. 7. Ratio factors for each user.

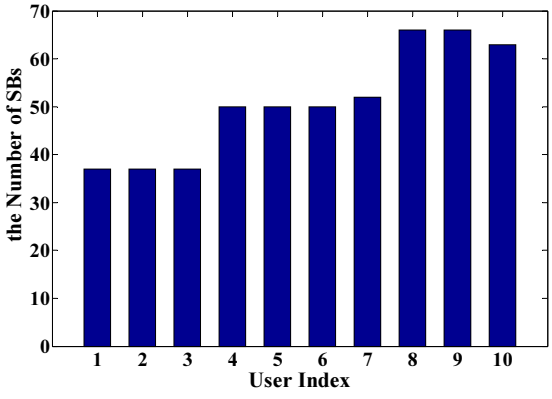

FIG. 8. The number of SB allocated to each user.

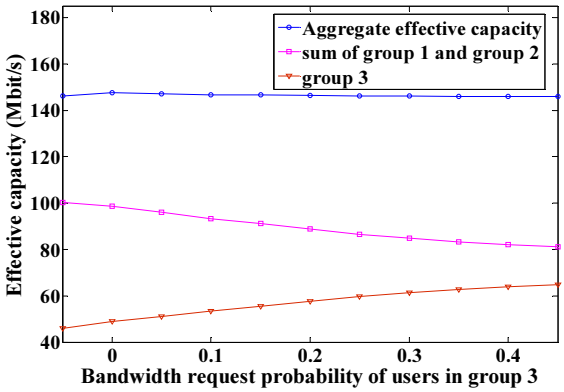

FIG. 9. The effective capacity of group 3, the sum of the effective capacity of group 1 and group 2, and the aggregate effective capacity versus the bandwidth request probability α of group 3.

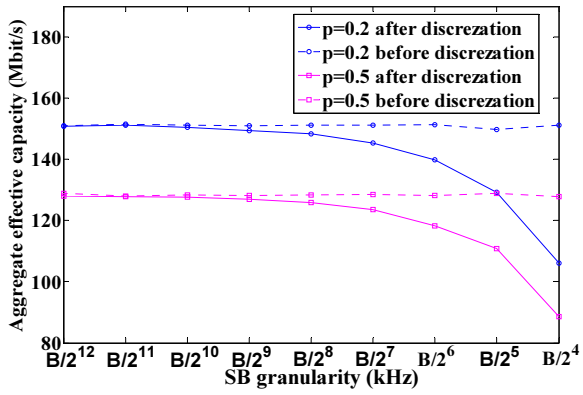

FIG. 10. The effect of SB granularity on the aggregate effective capacity.

after discretization decreases as SB granularity increases, and it approaches the aggregate effective capacity before discretization when the SB granularity is smaller than B/2[9] kHz. In fact, the gap between the aggregate effective capacity before and after discretization is affected by the discretization precision of $\underline{L}_k$ which is determined by SB granularity. A smaller SB granularity implies a higher discretization precision, which contributes to a smaller gap. Additionally, a smaller gap indicates smaller reduction of bandwidth utilization, as shown in Fig. 10, a smaller SB granularity implies smaller reduction of bandwidth utilization.

VI. CONCLUSION

In this paper, we have investigated the BA problem in the downlink of a VLC-OFDM system under multi-level service guarantees. Effective capacity theory is used to characterize the system capacity. Since an IM/DD technique is utilized in the system, the difference between SBs allocated to a user can be ignored. Therefore, the BA problem can be formulated as an integer programming problem. We relax the integer condition and have proved mathematically that the relaxed problem is a concave one. Lagrangian formulation is used to reformulate the concave problem. Considering the inefficiency of the traditional gradient-based schemes and the demand for distributed implementation in local area networks, we localized the global parameters and propose a quasi-distributed algorithm which is a quadratic allocation scheme, the first one is QoS oriented, and the second one is QoE oriented. Our simulation demonstrates that the quasi-distributed scheme can converge to the suboptimal solution within small epochs. By comparing with the average bandwidth allocation scheme, the BA scheme can achieve a greater aggregate effective capacity, and the advantages are getting greater as the QoS requirements are getting more stringent. The VLC system is sensitive to the delay constraints, and the aggregate effective capacity degrades rapidly for$\theta \geq 0.1$. More SBs are assigned to the users with larger delay exponent θ to guarantee their delay QoS constraint. The bandwidth request probability affects the distribution of SBs, but has no effect on the aggregate effective capacity of the system. The discretization of $\underline{L}_k$ reduces the bandwidth utilization. The aggregate effective capacity increases as the SB granularity decreases.

APPENDIX A

The first derivative of the effective capacity C_E^k from the VLC link for terminal k is given by:

$$\frac{\partial C_E^k(\beta_k)}{\partial \beta_k} = \frac{(1-p_k)R_{1,k}e^{-\theta_k\beta_k R_{1,k}} + p_k R_{2,k}e^{-\theta_k\beta_k R_{2,k}}}{(1-p_k)e^{-\theta_k\beta_k R_{1,k}} + p_k e^{-\theta_k\beta_k R_{2,k}}}$$

The second derivative of the effective capacity C_E^k from the VLC link for terminal k is given by:

$$\frac{\partial^2 C_E^k(\beta_k)}{\partial \beta_k^2} = -\frac{p_k(1-p_k)\theta_k(R_{1,k}-R_{2,k})^2 e^{-\theta_k\beta_k(R_{1,k}+R_{2,k})}}{[(1-p_k)e^{-\theta_k\beta_k R_{1,k}} + p_k e^{-\theta_k\beta_k R_{2,k}}]^2}$$

Since $\theta_k \geq 0, 0 \leq p \leq 1$, we get $\frac{\partial^2 C_E^k(\beta_k)}{\partial \beta_k^2} \leq 0$. As a result, the objective function of Problem 2 is a concave function with respect to β_k.

APPENDIX B

The first derivative of the effective capacity C_E^k respect to the variable β_k is:

$$\frac{\partial C_E^k(\beta_k)}{\partial \beta_k} = \frac{(1-p_k)R_{1,k}e^{-\theta_k\beta_k R_{1,k}} + p_k R_{2,k}e^{-\theta_k\beta_k R_{2,k}}}{(1-p_k)e^{-\theta_k\beta_k R_{1,k}} + p_k e^{-\theta_k\beta_k R_{2,k}}} \tag{19}$$

Substituting (19) into (12), we can get:

$$\begin{aligned}(1-p_k)R_{1,k}e^{-\theta_k\beta_k R_{1,k}} + p_k R_{2,k}e^{-\theta_k\beta_k R_{2,k}} \\ = A_k((1-p_k)e^{-\theta_k\beta_k R_{1,k}} + p_k e^{-\theta_k\beta_k R_{2,k}})\end{aligned} \tag{20}$$

Since $e^{-\theta_k\beta_k R_{2,k}} > 0$, (20) can be converted into :

$$(1-p_k)(R_{1,k}-A_k)e^{-\theta_k\beta_k(R_{1,k}-R_{2,k})} = p_k(A_k - R_{2,k})$$

We assume that $0 < p < 1$, when $R_{2,k} < A_k < R_{1,k}$, we can get the closed-form of the optimal solution β_k :

$$\beta_k = \frac{1}{-\theta_k(R_{1,k}-R_{2,k})}\ln\frac{p_k(A_k-R_{2,k})}{(1-p_k)(R_{1,k}-A_k)}$$

Additionally, the first derivative of β_k^* with respect to A_k can be expressed as:

$$\frac{\partial \beta_k^*}{\partial A_k} = \frac{1}{-\theta_k(A_k-R_{2,k})(R_{1,k}-A_k)}$$

where $R_{2,k} < A_k < R_{1,k}$ and $\theta_k > 0$, we get $\frac{\partial \beta_k^*}{\partial A_k} < 0$ which implies that β_k^* is monotonic decreasing with A_k. Since $0 \leq \beta_k^* \leq 1$, the feasible region of A_k is expressed as:

$$A_k \in [\frac{p_k R_{2,k} + \xi(1-p_k)R_{1,k}}{p_k + \xi(1-p_k)}, p_k R_{2,k} + (1-p_k)R_{1,k}]$$

where $\xi = e^{-\theta(R_{1,k}-R_{2,k})}$.

REFERENCE

1. A. T. Hussein and J. M. H. Elmirghani, "Mobile multi-gigabit visible light communication system in realistic indoor environment," J. Lightwave Technol. **33**, 3293-3307 (2015).
2. Z. Wang, Y. Liu, Y. Lin, and S. Huang, "Full-duplex MAC protocol based on adaptive contention window for visible light communication," IEEE J. Opt. Commun. Netw. **7**, 164-171 (2015).
3. J. Dang and Z. Zhang, "Comparison of optical OFDM-IDMA and optical OFDMA for uplink visible light communications," in *Proc. 2012 International Conference on Wireless Communications and Signal Processing* (Huangshan, China, Oct. 2012), vol. 7363, pp. 1-6.
4. Y. S. Cho, *Wireless Communications with MATLAB* (Wiley Press, Singapore, 2010).
5. K. Yun, C. Lee, K. I. Ahn, R. Lee, and J. S. Jang, "Optimal signal amplitude of orthogonal frequency-division multiplexing systems in dimmable visible light communications," J. Opt. Soc. Korea. **18**, 459-465 (2014).
6. M. Kashef, M. Abdallah, and K. Qaraqe, "Power allocation for downlink multi-user SC-FDMA visible light communication systems," in *Proc. 49th Annual Conference on Information Sciences and Systems* (Baltimore, MD, United states, March. 2015), pp. 1-5.
7. Q. Lu, X. Ji, and K. Huang, "Clipping distortion analysis and optimal power allocation for ACO-OFDM based visible light communication," in *Proc. 4th IEEE International Conference on Information Science and Technology* (Shenzhen, China, Apr. 2014), pp. 320-323.
8. Y. Wang and N. Chi, "Asynchronous multiple access using flexible bandwidth allocation scheme in SCM-based 32/64QAM-OFDM VLC system," Photonic. Netw. Commun. **27**, 57-64 (2014).
9. J. Yuan and Q. Wang, "Delay quality-of-service driven resource allocation for relay-based multiuser OFDMA networks," in *Proc. IEEE International Conference on Communications 2012* (Ottawa, ON, Canada, Jun. 2012), pp. 3889- 3894.
10. X. Bao, G. Yu, J. Dai, and X. Zhu, "Li-Fi: Light fidelity-a survey," Wirel. Netw. **21**, 1879-1889 (2015).
11. Y. Wang, Y. Wang, and L. Wang, "Providing QoS guarantee for real-time service in wireless OFDM networks with effective capacity Method," in *Proc. 2007 International Conference on Wireless Communications, Networking and Mobile Computing* (Shanghai, China, Sep. 2007), pp. 1988-1991.
12. A. Aijaz, M. Tshangini, M. R. Nakhai, X. Chu, and A. H. Aghvami, "Energy-efficient uplink resource allocation in LTE networks with M2M/H2H co-Existence under statistical QoS guarantees," IEEE Trans. Commun. **62**, 2353-2365 (2014).
13. F. Jin, R. Zhang, and L. Hanzo, "Resource allocation under delay-guarantee constraints for heterogeneous visible-light and RF femtocell," IEEE Trans. Wireless Commun. **14**, 1020-1034 (2015).
14. L. Zhao, X. Chi, and W. Shi, "A QoS-driven random access algorithm for MPR-capable VLC system," IEEE Commun. Lett. **pp**, 1-1 (2016).
15. Y. Wang, D. A. Basnayaka, and H. Haas, "Dynamic load balancing for hybrid Li-Fi and RF indoor networks," in *Proc. 2015 IEEE International Conference on Communication Workshop* (London, UK, Jun. 2015), pp. 1422-1427.
16. K. Lee K, H. Park, and J. R. Barry, "Indoor channel characteristics for visible light communications," IEEE Commun. Lett. **15**, 217-219 (2011).
17. T. Komine and M. Nakagawa, "Fundamental analysis for visible-light communication system using LED lights," IEEE Trans. Consum. Electron, **50,** 100-107 (2004).
18. R. Mesleh, H. Elgala, and H. Haas, "LED nonlinearity mitigation techniques in optical wireless OFDM communication systems," IEEE J. Opt. Commun. Netw. **4**, 865-875 (2012).
19. J. M. Kahn and J. R. Barry, "Wireless infrared communications," P. IEEE. **85**, 265-298 (1997).
20. D. Wu and R. Negi, "Effective capacity: a wireless link model for support of quality of service," IEEE Trans. Wireless Commun. **2**, 630-643 (2003).
21. J. Tang and X. Zhang, "Cross-layer-model based adaptive resource allocation for statistical QoS guarantees in mobile wireless networks," IEEE Trans. Wireless Commun. **7,** 2318-2328 (2008).
22. S. Boyd and L. Vandenberghe, *Convex Optimization* (Cambridge University Press, UK, 2004).
23. D. P. Palomar and M. A. Chiang, "A tutorial on decomposition methods for network utility maximization," IEEE J. Sel. Areas. Commun. **24**, 1439-1451 (2006).